• Clinical Research •

Scanning-slit topography in patients with keratoconus

László Módis Jr.[1], Gábor Németh[2], Eszter Szalai[1], Zsuzsa Flaskó[1], Berthold Seitz[3]

[1]Department of Ophthalmology, University of Debrecen, Medical and Health Science Center, Debrecen 4032, Hungary

[2]Borsod-Abaúj-Zemplén County Hospital and University Teaching Hospital, Miskolc 3526, Hungary

[3]Department of Ophthalmology, Homburg Keratoconus Center, University of Saarland, Homburg/Saar 66424, Germany

Correspondence to: Gabor Nemeth. Borsod-Abaúj-Zemplén County Hospital and University Teaching Hospital, Miskolc 3526, Hungary. nemeth222@yahoo.com

Received: 2016-08-08   Accepted: 2016-12-06

Abstract

● AIM: To evaluate the anterior and posterior corneal surfaces using scanning-slit topography and to determine the diagnostic ability of the measured corneal parameters in keratoconus.

● METHODS: Orbscan II measurements were taken in 39 keratoconic corneas previously diagnosed by corneal topography and in 39 healthy eyes. The central minimum, maximum, and astigmatic simulated keratometry (K) and anterior axial power values were determined. Spherical and cylindrical mean power diopters were obtained at the central and at the steepest point of the cornea both on anterior and on posterior mean power maps. Pachymetry evaluations were taken at the center and paracentrally in the 3 mm zone from the center at a location of every 45 degrees. Receiver operating characteristic (ROC) analysis was used to determine the best cut-off values and to evaluate the utility of the measured parameters in identifying patients with keratoconus.

● RESULTS: The minimum, maximum and astigmatic simulated K readings were 44.80±3.06 D, 47.17±3.67 D and 2.42±1.84 D respectively in keratoconus patients and these values differed significantly (*P*<0.0001 for all comparisons) from healthy subjects. For all pachymetry measurements and for anterior and posterior mean power values significant differences were found between the two groups. Moreover, anterior central cylindrical power had the best discrimination ability (area under the ROC curve=0.948).

● CONCLUSION: The results suggest that scanning-slit topography and pachymetry are accurate methods both for keratoconus screening and for confirmation of the diagnosis.

● KEYWORDS: keratoconus; Orbscan; topography; pachymetry

INTRODUCTION

Keratoconus is a bilateral corneal ectasia characterized by progressive stromal thinning, protrusion of the corneal surface and topographic alterations[1]. Keratoconus has been traditionally classified as a noninflammatory disease[2], however recently non-inflammatory theory has been raised[3]. The prevalence varies substantially by ethnic groups, age, and gender from 0.007% (6.8 patients per 100 000 population) to 2.34%[4-8]. Besides the well-described clinical signs corneal topography and pachymetry-tomography-evaluations are essential in diagnosing and in the follow-up in patients of keratoconus.

The Orbscan slit-scanning topography system was one of the first instruments on the market with the ability to yield corneal thickness, curvature and elevation data simultaneously since its introduction in 1995[9-10]. Orbscan has been applied in several conditions, including in management of ophthalmic[11-13] and systematic disorders[14], as well as in preoperative surgical planning and postoperative monitoring the effect of refractive[15-19] and cataract procedures[20-21] on the anterior segment of the eye. The aim of the present study was to evaluate the anterior and posterior corneal surfaces using the Orbscan II topography instrument in keratoconic subjects. We determined topographic features and shape of the diseased corneas, central and paracentral corneal thicknesses and compared the results to healthy eyes. The ability of the corneal parameters to differentiate between keratoconic and healthy eyes was also studied.

SUBJECTS AND METHODS

The study followed the Declaration of Helsinki and all subjects signed informed consent regarding the examinations.

A total of seventy-eight subjects were enrolled in this study. Orbscan II corneal topography (Bausch & Lomb Surgical, Orbtek Inc., Salt Lake City, Utah, USA) examinations were conducted in thirty-nine eyes of 39 patients (with a mean age of 26.26±5.43y). Patients were previously diagnosed with keratoconus according to video keratoscopic characteristics and stromal thinning. Thirty-nine control subject (with a mean

Table 1 The anterior and posterior corneal power measurements

Orbscan data	Subjects		P^2
	Normal (*n*=39)	Keratoconus (*n*=39)	
Anterior axial corneal power[1]			
Central	48.90±2.33 (48.14-49.65)	56.87±5.70 (55.02-58.72)	<0.0001
Steepest	51.19±2.50 (59.20-63.47)	61.33±6.58 (59.20-63.47)	<0.0001
Anterior mean corneal power[1]			
Central spherical	49.25±2.74 (48.36-50.14)	56.20±5.12 (54.55-57.87)	<0.0001
Central cylindrical	2.12±0.86 (1.84-2.40)	6.23±2.60 (5.38-7.07)	<0.0001
Steepest spherical	51.00±2.17 (50.30-51.71)	60.75±6.79 (58.55-62.95)	<0.0001
Steepest cylindrical	2.12±0.66 (1.90-2.33)	4.58±2.02 (3.93-5.23)	<0.0001
Posterior mean corneal power[1]			
Central spherical	-6.48±0.65 (-6.70 to -6.27)	-7.60±2.66 (-8.47 to -6.74)	<0.0001
Central cylindrical	-0.76±0.62 (-0.96 to -0.56)	-1.79±0.77 (-2.04 to -1.54)	<0.0001
Steepest spherical	-7.14±0.56 (-7.32 to -6.96)	-9.16±1.48 (-9.64 to -8.68)	<0.0001
Steepest cylindrical	-0.94±0.88 (-1.23 to -0.66)	-1.26±0.58 (-1.44 to -1.07)	0.001

[1]Mean±standard deviation (95% confidence interval) (D); [2]Results of Mann-Whitney test between normal and keratoconus groups.

age of 65.23±13.75y) were also recruited (one eye per subject) who had negative history and signs of previous or present ocular disease. Contact lens wearers were excluded. Corneas with extensive refractive error over ±4.0 diopters (D) spherical and 3.0 D cylindrical power were also excluded from the study. Slit-scanning topography maps were recorded and the central minimum, maximum, and astigmatic simulated keratometry (K) and anterior axial power values were determined. To describe the corneal shape, the elevation data at the center and at the steepest location of the cornea on the anterior and posterior best-fit sphere maps were recorded. The spherical and cylindrical mean power diopters were obtained at the central and at the steepest point of the cornea on both anterior and posterior mean power maps. The steepest points on each map were defined by one experienced investigator using the cursor. Finally, pachymetry measurements were taken at the center and paracentrally, in the 3 mm zone from the center at a location of every 45 degrees. The thinnest and the average thickness of the cornea were automatically determined by the Orbscan system.
Statistical Analysis Statistical analysis was performed with the SPSS 13 version for Windows and MedCalc 10 version. Descriptive statistical results were described as mean, standard deviation and 95% confidence interval (95% CI) for the mean values. Comparisons between groups or variables were performed using the Mann-Whitney unpaired test. For correlation analysis, Spearman's rank test was carried out. Receiver operating characteristic (ROC) curves were created displaying the accuracy of the different corneal parameters in screening and confirmation for keratoconus. ROC analysis was applied to determine the optimal cut-off values and to evaluate the performance of the measured parameters to distinguish keratoconic eyes from normals. Sensitivity, specificity, positive and negative predictive values for each cut-off were

also calculated. For screening keratoconus, we selected cut-off values with the highest possible specificity and negative predictive value, and with optimal sensitivity. To confirm diagnosis of the disease, threshold values with maximal specificity and positive predictive value were also yielded. A *P* value less than 0.05 was considered statistically significant.

RESULTS
For keratoconus patients, the minimum, maximum and astigmatic simulated K value were 44.80±3.06 D, 47.17±3.67 D and 2.42±1.84 D, and differed significantly (*P*<0.0001 for all comparisons) from those values of control subjects (42.25±1.77 D, 43.84±2.39 D and 1.04±0.80 D, respectively). The corneal power measurements obtained in the normal and keratoconic eyes are summarized in Table 1. Statistically significant differences were disclosed in the anterior axial power results between the two patients groups (*P*<0.0001). Both for the anterior and posterior surfaces, significant differences were found in the spherical and cylindrical power readings at the center and the steepest point between normal and diseased corneas. In keratoconus patients, Spearman's rank test detected significant negative correlation between the anterior and posterior spherical mean power values at the steepest location (*r*=-0.768, *P*<0.0001), at the central point (*r*=-0.858, *P*<0.0001), as well as between the anterior and posterior cylindrical mean power at the steepest location (*r*=-0.335, *P*=0.037) and at the central point (*r*=-0.545, *P*<0.0001). In the control group, the anterior mean spherical power correlated significantly with the posterior mean spherical power both at the steepest and central location (*r*=-0.442, *P*=0.001; *r*=-0.269, *P*=0.047, respectively). We detected statistical significant differences in the elevation values both on the anterior and posterior surfaces between the healthy and diseased groups (*P*<0.0001) (Table 2).

Table 2 Elevation of the anterior and posterior corneal surfaces reflected by the best-fit sphere measurements

Orbscan data	Subjects		P[2]
	Normal (*n*=39)	Keratoconus (*n*=39)	
Anterior best-fit sphere, center[1]	0.0098±0.0074 (0.0074-0.0122)	0.0371±0.0222 (0.0299-0.0443)	<0.0001
Anterior best-fit sphere, steepest[1]	0.0153±0.0128 (0.0111-0.0194)	0.057±0.0311 (0.0469-0.0671)	<0.0001
Posterior best-fit sphere, center[1]	0.0225±0.0144 (0.0179-0.0272)	0.0646±0.0437 (0.0504-0.0787)	<0.0001
Posterior best-fit sphere, steepest[1]	0.0349±0.0227(0.0275-0.0423)	0.105±0.0588 (0.0863-0.124)	<0.0001

[1]Mean±standard deviation (95% confidence interval) (mm); [2]Results of Mann-Whitney test between normal and keratoconus groups.

Table 3 Corneal thickness measurements obtained at the center and the paracentral zone

Corneal thickness	Subjects		P[3]
	Normal (*n*=39)	Keratoconus (*n*=39)	
Thinnest[1]	582.59±48.61 (566.83-598.35)	470.10±76.66 (445.25-494.95)	<0.0001
Central[1]	597.87±52.81 (580.75-614.99)	511.82±56.27 (493.58-530.06)	<0.0001
Temporal[2]	654.26±55.60 (636.23-672.28)	589.64±35.51 (578.13-601.15)	<0.0001
Superotemporal[1,2]	664.49±52.92 (647.33-681.64)	622.56±34.38 (611.42-633.71)	<0.0001
Superior[1,2]	670.21±50.78 (653.75-686.67)	645.72±39.19 (633.02-658.42)	0.013
Superonasal[1,2]	662.36±50.48 (645.99-678.72)	642.26±38.40 (629.81-654.71)	0.027
Nasal[1,2]	667.62±51.17 (651.03-684.20)	632.00±47.66 (616.55-647.45)	0.002
Inferonasal[1,2]	674.41±42.16 (660.74-688.08)	634.36±64.76 (613.37-655.35)	0.001
Inferior[1,2]	666.33±43.34 (652.29-680.38)	623.54±48.31 (607.88-639.20)	<0.0001
Inferotemporal[1,2]	658.26±46.28 (643.25-673.26)	593.26±45.02 (578.66-607.85)	<0.0001

[1]Mean±standard deviation (95% confidence interval) (μm); [2]3 mm from the center; [3]Results of Mann-Whitney test between normal and keratoconus groups. For all pachymetry measurements, significant differences were found between normal and keratoconus subjects.

Regarding corneal thickness measurements, in healthy and keratoconic eyes, the thinnest part of the cornea was found temporally. In keratoconus eyes pachymetry results were the highest in the superior corneal region. In healthy and keratoconic eyes the corneal thicknesses were significantly different from the superior nasal (3.46 μm, *P*=0.032), inferior (22.18 μm, *P*=0.009), superior temporal (23.16 μm, *P*<0.0001) and temporal (56.08 μm, *P*<0.0001) quadrants (Table 3).

Figure 1 shows the scanning-slit pachymetry measurements at the center, at the thinnest point and paracentrally. In both study groups the central cornea was significantly thinner than the paracentral values in a 3 mm zone (*P*<0.0001).

On the basis of ROC curve analysis (Table 4 and Figure 2), anterior central cylindrical power had the best screening ability [area under the ROC curve (AUROC)=0.948] followed by: anterior steepest spherical power (0.936), anterior elevation at the steepest location (0.925), posterior steepest spherical power (0.911) and thinnest pachymetry (0.906). Threshold values with maximal specificity and positive predictive value for corneal parameters with the best diagnostic accuracy are shown in Table 5.

DISCUSSION

Elevation-based corneal topography instruments are capable of imaging the true shape of the cornea. The PAR Technology Corneal Topography System was the first development based on elevation topography that provided 3D surface data only
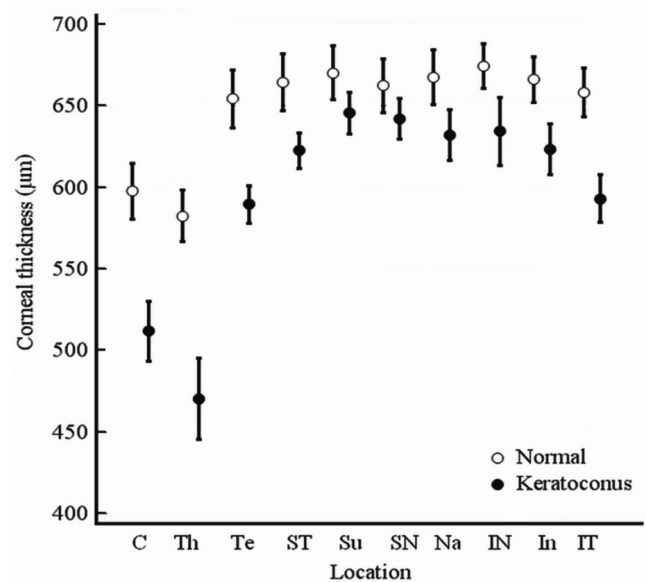

Figure 1 Scanning-slit pachymetry measurements at the center (C), at the thinnest point (Th) and paracentrally Te: Temporally; ST: Superotemporally; Su: Superior; SN: Superonasally; Na: Nasally; IN: Inferonasally; In: Inferior; IT: Inferotemporally.

on the anterior cornea[22]. Additional 3D topographers such as Orbscan I can measure both the front and back corneal elevation and convert height parameters to curvature data. The second generation of Orbscan system (Orbscan II) operates as a slit-scanning topographer combined with the Placido disk technique and captures particularly corneal curvature

Table 4 ROC curve analysis for screening keratoconus

ROC curve data	AUROC (95% CI)	SE	Cut-off	Sensitivity[1]	Specificity[1]	PPV[1]	NPV[1]
Anterior mean corneal power							
Central spherical	0.893[a] (0.803-0.952)	0.0376	>52.12 D	76.92 (60.7-88.8)	89.74 (75.8-97.1)	88.2 (72.5-96.6)	79.5 (64.7-90.2)
Central cylindrical	0.948[a] (0.872-0.985)	0.0264	>3.52 D	82.05 (66.5-92.4)	94.87 (82.6-99.2)	94.1 (80.3-99.1)	84.1 (69.9-93.3)
Steepest spherical	0.936[a] (0.857-0.979)	0.0292	>53.08 D	87.18 (72.6-95.7)	89.74 (75.8-97.1)	89.5 (75.2-97.0)	87.5 (73.2-95.8)
Steepest cylindrical	0.881[a] (0.787-0.943)	0.0397	>2.61 D	82.05 (66.5-92.4)	84.62 (69.5-94.1)	84.2 (68.7-93.9)	82.5 (67.2-92.6)
Posterior mean corneal power							
Central spherical	0.861[a] (0.764-0.929)	0.0428	≤-7.46 D	64.10 (47.2-78.8)	97.44 (86.5-99.6)	96.2 (80.3-99.4)	73.1 (59.0-84.4)
Central cylindrical	0.877[a] (0.783-0.941)	0.0403	≤-0.88 D	92.31 (79.1-98.3)	74.36 (57.9-86.9)	78.3 (63.6-89.0)	90.6 (75.0-97.9)
Steepest spherical	0.911[a] (0.824-0.963)	0.0345	≤-7.83 D	76.92 (60.7-88.8)	92.31 (79.1-98.3)	90.9 (75.6-98.0)	80.0 (65.4-90.4)
Steepest cylindrical	0.727[a] (0.614-0.822)	0.0573	≤-0.66 D	87.18 (72.6-95.7)	56.41 (39.6-72.2)	66.7 (52.1-79.2)	81.5 (61.9-93.6)
Elevation							
Anterior central	0.884[a] (0.792-0.946)	0.0391	>0.01 mm	79.49 (63.5-90.7)	79.49 (63.5-90.7)	79.5 (63.5-90.7)	79.5 (63.5-90.7)
Anterior steepest	0.925[a] (0.843-0.972)	0.0316	>0.02 mm	87.18 (72.6-95.7)	94.87 (82.6-99.2)	94.4 (81.3-99.2)	88.1 (74.4-96.0)
Posterior central	0.843[a] (0.742-0.915)	0.0453	>0.03 mm	76.92 (60.7-88.8)	82.05 (66.5-92.4)	81.1 (64.8-92.0)	78.0 (62.4-89.4)
Posterior steepest	0.883[a] (0.790-0.945)	0.0394	>0.05 mm	79.49 (63.5-90.7)	89.74 (75.8-97.1)	88.6 (73.2-96.7)	81.4 (66.6-91.6)
Corneal thickness							
Center	0.870[a] (0.775-0.935)	0.0414	≤548 μm	74.36 (57.9-86.9)	82.05 (66.5-92.4)	80.06 (64.0-91.8)	76.2 (60.5-87.9)
Thinnest	0.906[a] (0.818-0.960)	0.0354	≤522 μm	76.92 (60.7-88.8)	87.18 (72.6-95.7)	85.7 (69.7-95.1)	79.1 (64.0-89.9)
Temporal	0.827[a] (0.725-0.904)	0.0473	≤640 μm	92.31 (79.1-98.3)	61.54 (44.6-76.6)	70.6 (56.2-82.5)	88.9 (70.8-97.5)
Superior	0.664 (0.548-0.767)	0.0614	≤646 μm	58.97 (42.1-74.4)	74.36 (57.9-86.9)	69.7 (51.3-84.4)	64.4 (48.8-78.1)
Nasal	0.708[a] (0.595-0.806)	0.0587	≤675 μm	89.74 (75.8-97.1)	48.72 (32.4-65.2)	63.6 (49.6-76.2)	82.6 (61.2-94.9)
Inferior	0.755[a] (0.645-0.846)	0.0549	≤669 μm	87.18 (72.6-95.7)	56.41 (39.6-72.2)	66.7 (52.1-79.2)	81.5 (61.9-93.6)

Optimal cut-offs for screening keratoconus based on different parameters. AUROC: Area under the ROC curve; SE: Standard error; PPV: Positive predictive value; NPV: Negative predictive value; 95% CI: 95% confidence interval. [1]Values in % with 95% CI; [a] Results of significance test below 0.05.
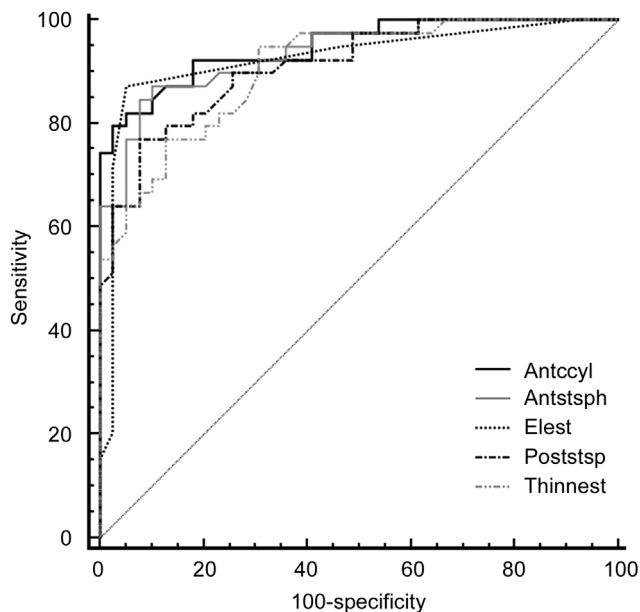
Figure 2 ROC curves for corneal parameters with the best diagnostic ability Antccyl: Anterior central cylindrical power; Antstsph: Anterior steepest spherical power; Elest: Anterior elevation at the steepest location; poststsp: Posterior steepest spherical power; Thinnest: Thinnest pachymetry.

readings, then translate these parameters into anterior and posterior elevation maps[9-10]. Orbscan not always perform well in corneas that are not normal, which can be mentioned as a limitation in our study. However, this is true for other topographic devices[23]. The rotating Scheimpflug imaging techniques such as Pentacam and Galilei perform corneal topographic analysis based on true elevation assessments from limbus to limbus. Elevation maps allow the clinicians to observe corneal abnormalities caused by either ectatic disorders (keratoconus, keratoglobus, pellucid marginal degeneration, posterior keratoconus) or acquired keratectasia after refractive procedures[17,24-30]. Today, the modern diagnostic methods for keratoconus includes Scheimpflug imaging, swept-source anterior segment optical coherence tomography (OCT), as well as biomechanical measurements, aimed to differentiate subclinical cases from normal corneas[31-33].

There are available literature data about comparison between Orbscan, Pentacam and swept-source OCT regarding normal and keratoconus corneas. One of these concluded that Scheimpflug camera and swept-source OCT showed statistically different output, but they have a good agreement in most measured corneal parameters[34]. Another paper showed significant differences in posterior corneal surface and corneal thickness measurements between swept-source OCT and a Scheimpflug camera in eyes with keratoconus, with better repeatability of measurements in case of the swept-source OCT[35]. Regarding corneal thickness measurements, swept source OCT, Pentacam and Orbscan II showed different data, with high correlation to each other[36].

Table 5 Cut-off values with maximal specificity and positive predictive value for the corneal parameters with the best discrimination ability

Cut-off values	Cut-off	Sensitivity[1]	Specificity[1]	PPV[1]	NPV[1]
Anterior central cylindrical power	>4.44 D	74.36 (57.9-86.9)	100 (90.9-100.0)	100 (87.9-100.0)	79.6 (65.7-89.7)
Anterior steepest spherical power	>56.36 D	64.1 (47.2-78.8)	100 (90.9-100.0)	100 (86.2-100.0)	73.6 (59.7-84.7)
Anterior steepest elevation	>0.03 mm	71.79 (55.1-85 .0)	97.44 (86.5-99.6)	96.6 (82.2-99.4)	77.6 (63.4-88.2)
Posterior steepest spherical power	≤-9.3 D	48.72 (32.4-65.2)	100 (90.9-100.0)	100 (82.2-100.0)	66.1 (52.6-77.9)
Thinnest pachymetry	≤480 μm	53.85 (37.2-69.9)	100 (90.9-100.0)	100 (83.7-100.0)	68.4 (54.8-80.1)

PPV: Positive predictive value; NPV: Negative predictive value; 95% CI: 95% confidence interval. [1]Values in % with 95% CI.

In the present study, Orbscan II evaluations were conducted on keratoconic eyes in comparison with normal healthy corneas. Both the axial and mean corneal power values on the anterior and posterior surfaces disclosed statistically significant difference between the two patients groups. Huang *et al*[37] emphasized that mean curvature map is superior to axial one in detecting and characterizing corneal ectasia since it is created by averaging two principal curvatures of the cornea point-by-point (*i.e.* locally), and astigmatic error is eliminated from these maps. For the anterior astigmatism, 4.11 D and 2.46 D difference was obtained at the center and the steepest location between the two groups; the posterior cylindrical power was also higher in the diseased group, the difference was 1.03 D in the center and 0.32 D at the steepest point. Moreover, anterior astigmatism at the corneal center yielded the highest AUROC (0.948) indicating the best ability to identify patients with keratoconus.

Orbscan determines the surface elevation relative to a reference shape (best-fit sphere). In the present study, radius of curvature of this reference body differed significantly in diseased and healthy eyes. A posterior elevation above 50 μm is suggested to identify as abnormal[27,38].

We also found a posterior elevation at the steepest location higher than 50 μm (with a sensitivity of 79.49%, specificity of 89.74%) and an anterior elevation higher than 20 μm (with a sensitivity of 87.18%, specificity of 94.87%) to be abnormal. A previous study reported a sensitivity of 57.7% and a specificity of 89.8% in differentiating keratoconus suspects and keratoconus from normal eyes when a posterior elevation higher than 40-50 μm was considered as abnormal[27]. In this study, sensitivity and specificity increased to 99.0% and 92.8%, respectively if making a distinction only between keratoconic and healthy corneas[27].

More recently, a cut-off point of ≥51 μm was specific (98.58%) and sensitive (89.23%) for posterior corneal elevation and a cut-off point of ≥19 μm was highly specific (97.16%) and sensitive (93.85%) for anterior corneal elevation to differentiate clinical keratoconus from normal subjects[39]. Central and paracentral corneal thickness were also evaluated

in this study. Both for healthy and diseased eyes, cornea was the thinnest in the center. Paracentrally, the lowest pachymetry values were detected at the temporal quadrant in 31% of the normal and 54% of the keratoconus patients, at the inferotemporal region in 18% of healthy and 31% of diseased eyes. Two other studies found the thinnest point to be located at the inferotemporal and the inferior quadrant in cases of keratoconus corneas, although those data were recorded with OCT near to the limbus and in a 5 mm zone, respectively[40-41]. In normal eyes, slit-scanning topography measured the thinnest pachymetry values temporally and inferotemporally in a 3 mm distance from the center[42-44]. Corneal thickness at the thinnest location showed great utility (AUROC=0.906) to discriminate keratoconus, although the best cut-off for this parameter (≤522 μm with the highest possible specificity and negative predictive value given maximal sensitivity) was higher than those reported previously[41,45]. ROC curve analysis showed the cut-off of the thinnest pachymetry value to be ≤480 μm ensuring maximal specificity (with a sensitivity of 53.85%, specificity of 100%). A cut-off value with the highest specificity and positive predictive value is useful for confirmation but not for screening purposes.

In conclusion, based on the ROC analysis anterior central cylindrical power had the best screening ability for keratoconus, followed by anterior steepest spherical power, anterior elevation at the steepest location, posterior steepest spherical power and thinnest pachymetry value. In addition, anterior central cylindrical power, anterior and posterior spherical power at the steepest location, anterior corneal elevation and thinnest pachymetry values seem to have the highest differentiation ability between patients with keratoconus and normal subjects. These results suggest that Orbscan II topography system is an applicable instrument both for keratoconus screening and for confirmation of the diagnosis.

REFERENCES

1 Davidson AE, Hayes S, Hardcastle AJ, Tuft SJ. The pathogenesis of keratoconus. *Eye (Lond)* 2014;28(2):189-195.

2 Jun AS, Cope L, Speck C, Feng X, Lee S, Meng H, Hamad A, Chakravarti S. Subnormal cytokine profile in the tear fluid of keratoconus patients. *PLoS One* 2011;6(1):16437.

3 McMonnies CW. Inflammation and keratoconus. *Optom Vis Sci* 2015;92(2):e35-e41.

4 Millodot M, Shneor E, Albou S, Atlani E, Gordon-Shaag A. Prevalence and associated factors of keratoconus in Jerusalem: a cross-sectional study. *Ophthalmic Epidemiol* 2011;18(2):91-97.

5 Nielsen K, Hjortdal J, Aagaard Nohr E, Ehlers N. Incidence and prevalence of keratoconus in Denmark. *Acta Ophthalmol Scand* 2007;85(8):890-892.

6 Reeves SW, Ellwein LB, Kim T, Constantine R, Lee PP. Keratoconus in the medicare population. *Cornea* 2009;28(1):40-42.

7 Ljubic A. Keratoconus and its prevalence in Macedonia. *Maced J Med Sci* 2009;2(1):58-62.

8 Jonas JB, Nangia V, Matin A, Kulkarni M, Bhojwani K. Prevalence and associations of keratoconus in rural maharashtra in central India: the central India eye and medical study. *Am J Ophthalmol* 2009;148(5):760-765.

9 Crawford AZ, Patel DV, McGhee CN. Comparison and repeatability of keratometric and corneal power measurements obtained by Orbscan II, Pentacam, and Galilei corneal tomography systems. *Am J Ophthalmol* 2013;156(1):53-60.

10 Oliveira CM, Ribeiro C, Franco S. Corneal imaging with slitscanning and Scheimpflug imaging techniques. *Clin Exp Optom* 2011;94(1):33-42.

11 Sonmez B, Doan MP, Hamilton DR. Identification of scanning slit-beam topographic parameters important in distinguishing normal from keratoconic corneal morphologic features. *Am J Ophthalmol* 2007;143(3):401-408.

12 Lee BW, Jurkunas UV, Harissi-Dagher M, Poothullil AM, Tobaigy FM, Azar DT. Ectatic disorders associated with a claw-shaped pattern on corneal topography. *Am J Ophthalmol* 2007;144(1):154-156.

13 Sanchis-Gimeno JA, Herrera M, Sánchez-del-Campo F, Martínez-Soriano F. Differences in ocular dimensions between normal and dry eyes. *Surg Radiol Anat* 2006;28(3):267-270.

14 Drolsum L, Rand-Hendriksen S, Paus B, Geiran OR, Semb SO. Ocular findings in 87 adults with Ghent-1 verified Marfan syndrome. *Acta Ophthalmol* 2015;93(1):46-53.

15 Alió JL, Shabayek MH, Artola A. Intracorneal ring segments for keratoconus correction: long-term follow-up. *J Cataract Refract Surg* 2006;32(6):978-985.

16 Lombardo M, Lombardo G, Friend DJ, Serrao S, Terry MA. Long-term anterior and posterior topographic analysis of the cornea after deep lamellar endothelial keratoplasty. *Cornea* 2009;28(4):408-415.

17 Ha BJ, Kim SW, Kim SW, Kim EK, Kim TI. Pentacam and Orbscan II measurements of posterior corneal elevation before and after photorefractive keratectomy. *J Refract Surg* 2009;25(3):290-295.

18 Maldonado MJ, López-Miguel A, Nieto JC, Cano-Parra J, Calvo B, Alió JL. Reliability of noncontact pachymetry after laser in situ keratomileusis. *Invest Ophthalmol Vis Sci* 2009;50(9):4135-4141.

19 Birnbaum F, Schwartzkopff J, Böhringer D, Reinhard T. Penetrating keratoplasty with intrastromal corneal ring. A prospective randomized study. *Ophthalmologe* 2008;105(5):452-456.

20 Gelender H. Orbscan II-assisted intraocular lens power calculation for cataract surgery following myopic laser in situ keratomileusis (an American Ophthalmological Society thesis). *Trans Am Ophthalmol Soc* 2006;104:402-413.

21 Morkin MI, Hussain RM, Young RC, Ravin T, Dubovy SR, Alfonso EC. Unusually delayed presentation of persistent Descemet's membrane tear and detachment after cataract surgery. *Clin Ophthalmol* 2014;28(8):1629-1632.

22 Ambrósio R Jr, Belin MW. Imaging of the cornea: topography vs tomography. *J Refract Surg* 2010;26(11):847-849.

23 Guilbert E, Saad A, Elluard M, Grise-Dulac A, Rouger H, Gatinel D. Repeatability of keratometry measurements obtained with three topographers in keratoconic and normal corneas. *J Refract Surg* 2016; 32(3):187-192.

24 Rejdak R, Nowomiejska K, Haszcz D, Jünemann AG. Bilateral circumscribed posterior keratoconus: visualization by ultrasound biomicroscopy and slit-scanning topography analysis. *J Ophthalmol* 2012;2012:587075.

25 Walker RN, Khachikian SS, Belin MW. Scheimpflug photographic diagnosis of pellucid marginal degeneration. *Cornea* 2008;27(8):963-966.

26 Lim L, Wei RH, Chan WK, Tan DT. Evaluation of keratoconus in Asians: role of Orbscan II and Tomey TMS-2 corneal topography. *Am J Ophthalmol* 2007;143(3):390-400.

27 Fam HB, Lim KL. Corneal elevation indices in normal and keratoconic eyes. *J Cataract Refract Surg* 2006;32(8):1281-1287.

28 Ciolino JB, Belin MW. Changes in the posterior cornea after laser in situ keratomileusis and photorefractive keratectomy. *J Cataract Refract Surg* 2006;32(9):1426-1431.

29 Hashemi H, Mehravaran S. Corneal changes after laser refractive surgery for myopia: comparison of Orbscan II and Pentacam findings. *J Cataract Refract Surg* 2007;33(5):841-847.

30 Spadea L, Cantera E, Cortes M, Conocchia NE, Stewart CW. Corneal ectasia after myopic laser in situ keratomileusis: a long-term study. *Clin Ophthalmol* 2012;6:1801-1813.

31 Steinberg J, Katz T, Lücke K, Frings A, Druchkiv V, Linke SJ. Screening for keratoconus with new dynamic biomechanical in vivo scheimpflug analyses. *Cornea* 2015;34(11):1404-1412.

32 Steinberg J, Casagrande MK, Frings A, Katz T, Druchkiv V, Richard G, Linke SJ. Screening for subclinical keratoconus using swept-source fourier domain anterior segment optical coherence tomography. *Cornea* 2015;34(11):1413-1419.

33 Steinberg J, Aubke-Schultz S, Frings A, Hülle J, Druchkiv V, Richard G, KatzT, Linke SJ. Correlation of the KISA% index and Scheimpflug tomography in'normal', 'subclinical', 'keratoconus-suspect' and 'clinically manifest' keratoconus eyes. *Acta Ophthalmol* 2015;93(3):e199-e207.

34 Ghoreishi SM, Mortazavi SA, Abtahi ZA, Abtahi MA, Sonbolestan SA, Abtahi SH, Mohammadinia M, Isfahani KN. Comparison of Scheimpflug and swept-source anterior segment optical coherence tomography in normal and keratoconus eyes. *Int Ophthalmol* 2017;37(4):965-971.

35 Chan TCY, Biswas S, Yu M, Jhanji V. Comparison of corneal measurements in keratoconus using swept-source optical coherence tomography and combined Placido-Scheimpflug imaging. *Acta Ophthalmol* 2017;95(6):e486-e494.

36 Kumar M, Shetty R, Jayadev C, Dutta D. Comparability and repeatability of pachymetry in keratoconus using four noncontact techniques. *Indian J Ophthalmol* 2015;63(9):722-727.

37 Huang D, Tang M. Gaussian fitting on mean curvature maps of parameterization of corneal ectatic diseases. *United States Patent* 2009;7: 497575.

38 Belin MW. Pentacam accurately detects keratoconus, diagnostic imaging for refractive and cataract surgery. Available at: https://www. oculususa.com/downloads/oculus_advertorial_5.15.05.pdf. Accessed on July 15, 2010.

39 Jafarinasab MR, Shirzadeh E, Feizi S, Karimian F, Akaberi A, Hasanpour H. Sensitivity and specificity of posterior and anterior corneal elevation measured by orbscan in diagnosis of clinical and subclinical keratoconus. *J Ophthalmic Vis Res* 2015;10(1):10-15.

40 Haque S, Jones L, Simpson T. Thickness mapping of the cornea and epithelium using optical coherence tomography. *Optom Vis Sci* 2008;85(10):E963-976.

41 Li Y, Meisler DM, Tang M, Lu AT, Thakrar V, Reiser BJ, Huang D. Keratoconus diagnosis with optical coherence tomography pachymetry mapping. *Ophthalmology* 2008;115(12):2159-2166.

42 Hashemi H, Asgari S, Mehravaran S, Emamian MH, Shariati M, Fotouhi A. The distribution of corneal thickness in a 40- to 64-year-old population of Shahroud, Iran. *Cornea* 2011;30(12):1409-1413.

43 Rüfer F, Sander S, Klettner A, Frimpong-Boateng A, Erb C. Characterization of the thinnest point of the cornea compared with the central corneal thickness in normal subjects. *Cornea* 2009;28(2):177-180.

44 Rüfer F, Schröder A, Bader C, Erb C. Age-related changes in central and peripheral corneal thickness: determination of normal values with the Orbscan II topography system. *Cornea* 2007;26(1):1-5.

45 Steele TM, Fabinyi DC, Couper TA, Loughnan MS. Prevalence of Orbscan II corneal abnormalities in relatives of patients with keratoconus. *Clin Exp Ophthalmol* 2008;36(9):824-830.